
Analytic Torsion and Spectral Gap Capture Persistent-Laplacian Performance

Jernej Grlj

Department of Mathematics
University of Southern California
Los Angeles, CA 90089
grlj@usc.edu

Aaron D. Lauda

Department of Mathematics
Department of Physics
University of Southern California
Los Angeles, CA 90089
lauda@usc.edu

Abstract

While persistent Laplacians (PL) offer a richer geometric representation of data than persistent homology, utilizing their full eigenspectrum for learning tasks is often hampered by high dimensionality and the “varying length” problem across different filtration scales. We propose a compact spectral representation that distills the persistent Laplacian into three mathematically grounded invariants: Betti numbers, the spectral gap, and analytic torsion. Across benchmark datasets including MNIST, QM-3D, and SKEMPI WT, we demonstrate that this reduced feature space captures the essential predictive signal of the full spectrum, and in some cases outperforms it, while significantly reducing computational overhead and preventing the noise introduced by higher-frequency eigenvalues. Our results suggest that these invariants provide a principled, fixed-length interface between spectral geometry and topological learning.

1 Introduction

Persistent homology has become one of the central tools of topological data analysis, because it tracks the birth and death of homological features across scale. Its strength is also its limitation: by design, it records topology up to homological persistence, but not the finer geometric information that can continue to evolve even when the barcode does not. Once a cycle is born, for example, cycle size, heterogeneity, and internal organization may change substantially while its persistent homology remains unchanged. In this regime, Laplacian-based methods become a natural extension. They retain topological information within their harmonic sector, while their non-harmonic spectra record additional geometric and combinatorial structure invisible to barcodes alone Edelsbrunner et al. (2002); Mémoli et al. (2022); Wei and Wei (2025b).

A useful way to frame this is through the classical spectral question posed by Kac: “Can one hear the shape of a drum?” Kac (1966). While the spectrum does not uniquely determine shape Gordon et al. (1992), it encodes a remarkable breadth of geometry and dynamics. In Riemannian geometry, graph theory, and manifold learning, Laplace spectra govern oscillation, heat flow, diffusion, and multiscale structure. On graphs, the first nonzero eigenvalue already detects global connectivity, transport, and underlies spectral partitioning Fiedler (1973). Physically, it marks the first nontrivial frequency above the harmonic sector and therefore the slowest nontrivial diffusion scale visible to the operator. Small gap values indicate that a non-harmonic mode can be excited at low energy, which often reflects weak connectivity, near-degeneracy, or the presence of large-scale structure Fiedler (1973); Chung (1997). More broadly, Laplacian eigenvalues and eigenvectors drive diffusion maps, Laplacian eigenmaps, and random-walk-based representations of data Belkin and Niyogi (2003); Coifman et al. (2005); Schaub et al. (2020). From an algorithmic perspective, this means that the upper part of the spectrum

is not decorative. It often carries discriminative information about local geometry and multiscale organization.

This perspective extends naturally from graphs to simplicial complexes. Eckmann’s combinatorial Laplacians generalize the graph Laplacian to operators acting on higher-dimensional simplices Eckmann (1945). In this setting, the kernel of the q -Laplacian recovers q -dimensional homology, while the nonzero eigenvalues capture additional structure beyond Betti numbers. Persistent Laplacians transport this idea to pairs of simplicial complexes $K \hookrightarrow L$, thereby combining persistence with higher-order spectral analysis Mémoli et al. (2022). Their harmonic spectra recover persistent homology, but their non-harmonic spectra retain geometric information discarded by purely homological summaries Wei and Wei (2025b); Wang et al. (2020). This makes persistent Laplacians a natural candidate for topological learning pipelines that seek both multiscale topology and a quantitative description of how shape evolves across the filtration. However, while these methods have shown significant promise in biomolecular prediction and graph learning Davies et al. (2023); Wang et al. (2020), their adoption faces a significant computational bottleneck.

As noted in recent evaluations Davies et al. (2023); Xu et al. (2025), packing spectral data into feature vectors is inherently difficult because the size of the spectra varies across different homological dimensions and filtration parameters. Previous attempts to resolve this typically rely on truncating the spectrum to a fixed number of eigenvalues or utilizing basic statistical summaries (e.g., mean or variance). However, naive truncation is often counterproductive: as the number of eigenvalues increases, the precision of the model often decreases Davies et al. (2023). This suggests that the higher part of the spectrum, while rich in information, often presents as an undifferentiated and noisy vector that hinders standard learning architectures.

Introduced by Ray and Singer as an analytic counterpart of Reidemeister torsion, analytic torsion is built from an alternating product of Laplacian pseudo-determinants and therefore depends on the full nonzero spectrum rather than only the harmonic sector Ray and Singer (1971). The subsequent work of Cheeger and Müller established the fundamental equivalence between analytic torsion and Reidemeister torsion in the classical setting Cheeger (1979); Müller (1978). In particular, torsion is not an ad hoc spectral statistic: it is a mathematically principled bridge between topology and analysis, designed precisely to capture information beyond Betti numbers.

While analytic torsion has deep roots in topology and spectral geometry, it has not become a standard feature in topological data analysis. We argue that persistent Laplacians provide a natural setting in which to import this invariant: the harmonic sector recovers persistent homological information, and the spectral gap captures only the first positive eigenvalue. Meanwhile, the analytic torsion summarizes the contribution of *all* nonzero eigenvalues. This makes torsion a mathematically grounded and computationally attractive feature for learning tasks built on persistent spectral data.

1.1 Mathematical Feature Engineering.

The transition from raw spectral data to predictive performance is not merely a matter of dimensionality, but one of functional complexity. Extracting global geometric invariants from this spectrum, most notably the analytic torsion we study here, poses a significant challenge for generic machine learning models. Analytic torsion is a sophisticated, non-linear function of the entire non-harmonic spectrum, requiring the computation of alternating products of pseudodeterminants across varying homological degrees. For a model to “discover” this invariant from raw eigenvalues, it would have to implicitly learn complex algebraic operations that are numerically sensitive and global in nature.

By providing analytic torsion as a direct feature, we perform a form of mathematical feature engineering. We supply the model with high-level geometric primitives that would otherwise remain opaque within a high-dimensional, varying-length feature vector. Analytic torsion compresses the higher-frequency information into a single, principled quantity, allowing the model to bypass the noise and dimensionality issues inherent in raw spectral data.

For standard machine learning architectures, such as the Random Forests and Gradient Boosting Regressors utilized in this study, deriving this signal from a raw list of eigenvalues requires overcoming several significant functional hurdles:

- Isolating the harmonic sector: The model must correctly identify the varying number of zero eigenvalues (the Betti numbers) to determine the starting index of the non-harmonic spectrum.

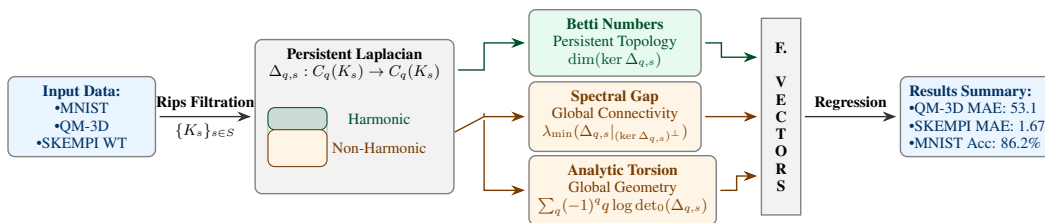


Figure 1: Conceptual pipeline for mathematical feature engineering using persistent Laplacians. The multi-scale persistent Laplacian $\Delta_{q,s}$, formed from Rips complexes, is decomposed into its harmonic and non-harmonic components. These contribute to the tripartite feature vectors consisting of Betti numbers, spectral gap, and analytic torsion. The results are obtained using appropriate regression methods.

- Computing multiplicative relationships: These models are inherently additive or based on axis-aligned splits; consequently, they struggle to approximate high-order multiplicative relationships, such as the product of all positive eigenvalues, without an explicit logarithmic transformation.
- Synthesizing across dimensions: The model would need to learn to integrate spectral data across multiple homological degrees q while correctly applying the alternating sign convention and exponentiation required by the torsion formula.

Supplying these primitives directly performs algorithmic offloading for the model. This bypasses the learning bottleneck, preserves critical structural information, and provides a universal, fixed-length interface. This approach also eliminates the guesswork and manual tuning typically required by truncation-based methods to identify thresholds of diminishing returns

1.2 Our Contributions.

Resolution of the Spectral Packing Problem We introduce a fixed-dimensional representation that resolves the inherent difficulty of utilizing varying-length spectral vectors across different homological dimensions and filtration parameters. This allows for a consistent input format for standard machine learning architectures without the need for heuristic truncation or basic statistical pooling.

A Principled Topological-Spectral Partitioning: We propose a novel feature set grounded in the structural decomposition of the persistent Laplacian. By utilizing the harmonic sector (Betti numbers) to capture persistent topology and spectral gap and analytic torsion to summarize the non-harmonic spectrum, we provide a mathematically rigorous alternative to naive eigenvalue vectorization.

Cross-Domain Empirical Robustness: We demonstrate the effectiveness of our topological-spectral representation across a widely varying suite of benchmarks, ranging from quantum mechanical properties of small molecules to large-scale protein engineering tasks and manifold learning in image datasets. Our results show that this mathematical feature reduction remains effective regardless of the underlying data dimensionality or domain-specific noise, and effectively circumvents the breaking point observed in previous studies, where increasing the number of raw eigenvalues leads to diminishing returns or decreased model precision Davies et al. (2023).

More broadly, our results support a simple thesis: the success of spectral methods in geometry, graph theory, and data analysis has always rested on the fact that nonzero eigenvalues encode meaningful structure. By utilizing the spectral gap to capture the leading nontrivial diffusion scale and analytic torsion to summarize the cumulative higher-frequency content, we offer a compact spectral interface between topology, geometry, and learning. This tripartite representation, comprising Betti numbers, the spectral gap, and analytic torsion, provides a principled, fixed-length summary that preserves the predictive power of the full persistent Laplacian while significantly reducing the noise and computational overhead associated with high-dimensional spectral data. In doing so, we establish a mathematically transparent framework for characterizing how shape and connectivity evolve across a filtration, effectively bridging the gap between classical spectral geometry and modern topological data analysis.

Organization of the paper

The remainder of this paper is organized as follows: Section 1.3 reviews related work in topological and spectral learning; Section 2 provides the necessary mathematical preliminaries on persistent Laplacians and torsion; Section 3 details our feature construction and computational considerations; and Section 4 presents our experimental results, ablation studies, and training times across various benchmarks.

1.3 Related Work

Vectorization of Topological Summaries: While persistent homology provides a robust multiscale summary of data Carlsson (2009), its raw outputs of persistence diagrams and barcodes are not natively compatible with standard machine learning kernels Davies et al. (2023). This limitation has motivated several vectorization frameworks, most notably Persistence Landscapes Bubenik (2015), Persistence Images Adams et al. (2017), and Persistence Silhouettes Chazal et al. (2015). These methods typically focus on functional or density-based summaries of birth-death pairs. While successful in many applications, these representations remain strictly homological; they inherit the limitation of ignoring the finer geometric and combinatorial evolution that occurs even when the barcode remains static. Our work with spectral invariants seeks to fill this gap by probing the geometry of the filtration that these density-based summaries omit.

Spectral Methods and Higher-Order Structure Our approach sits within a well-established tradition of using Laplacian spectra for representation learning in manifold learning Belkin and Niyogi (2003); Coifman et al. (2005), out-of-distribution robustness diagnostics Zia and Hazratian (2026), and graph theory Fiedler (1973). Foundational methods such as Laplacian eigenmaps and diffusion maps leverage low-frequency eigenvalues to detect global connectivity and coarse organization. These concepts extend from graphs to higher-order networks through Eckmann’s combinatorial Laplacians Eckmann (1945), where nonzero eigenvalues capture structural information and higher-order diffusion that Betti numbers alone cannot resolve Schaub et al. (2020). By extracting global invariants from these operators, we leverage this broader spectral-learning tradition to characterize multiscale organization in simplicial complexes.

Persistent Laplacians and Spectral Representations This paper builds on the persistent Laplacian (PL) framework introduced by Mémoli et al. Mémoli et al. (2022), which tracks the evolution of the non-harmonic spectrum across a filtration. Extensions of this work include the Persistent sheaf Laplacians Jones and Wei (2026); Wang and Wei (2026); Wei and Wei (2025a), persistent path Laplacians Wang and Wei (2023) and persistent hyperdigraph Laplacians Chen et al. (2023) for instance. Persistent Laplacians have already shown significant promise in practical applications, such as the projection of COVID-19 variants Chen et al. (2022) and protein-protein interaction prediction Xu et al. (2025); Wang et al. (2020). However, utilizing the full spectrum for learning introduces the “spectral packing” problem: the size of eigenspectra varies significantly across homological dimensions and filtration parameters Davies et al. (2023). Previous attempts to resolve this have relied on truncating the spectrum to a fixed number of eigenvalues Davies et al. (2023) or utilizing basic statistical descriptors like mean and standard deviation Xu et al. (2025). In a different direction Jung et al. (2025) studies the persistent Laplacian image as the vectorization of spectral information, generalizing Adams et al. (2017). Our results contribute to this effort by demonstrating that the spectral content can be compressed into principled invariants, Betti numbers, gaps, and torsion, without the noise or diminishing returns associated with naive truncation.

Torsion-Based Summaries Analytic torsion has deep roots in spectral geometry as a bridge between topology and analysis, originally developed by Ray and Singer Ray and Singer (1971) and further established by Cheeger and Müller Cheeger (1979); Müller (1978). While historically used for the classification of manifolds Reidemeister (1935), its use as a feature in modern learning pipelines remains an emerging frontier. Recent work has begun to integrate torsion into graph neural networks (GNNs) as a local weighting device within message-passing protocols Shen et al. (2025); Li et al. (2025). Our approach represents a distinct shift in methodology: rather than utilizing torsion for local architectural weighting, we treat it as a *global invariant* extracted directly from the persistent Laplacian. This allows us to import a classical topological invariant into a persistent spectral learning framework in a way that is both mathematically natural and algorithmically useful.

2 Preliminaries on Persistent Laplacians and Spectral Summaries

We present some minimal mathematical background needed to understand the problem at hand. For more details on persistent Laplacians, we refer the reader to Mémoli et al. (2022), and to Carlsson (2009) for the original work on persistent homology.

2.1 Simplicial complexes, chain groups, and boundary operators

A (finite, abstract) simplicial complex K on a vertex set V is a collection of finite subsets of V that is closed under taking subsets: if $\sigma \in K$ and $\tau \subseteq \sigma$, then $\tau \in K$. If σ has $q + 1$ vertices, then σ is called a q -simplex, and we write K_q for the set of all q -simplices in K . Thus, K_0 is the set of vertices, K_1 the set of edges, K_2 the set of triangles, and so on.

To define Laplacians, one passes from simplices to oriented chain groups. For each $q \geq 0$, let $C_q(K)$ denote the vector space of formal linear combinations of oriented q -simplices in K with coefficients in \mathbb{R} . Equivalently, after choosing an orientation for each simplex in K_q , the group $C_q(K)$ may be identified with $\mathbb{R}^{|K_q|}$. We write a typical basis element as $[v_0, v_1, \dots, v_q]$, where the ordering specifies the orientation, and reversing orientation changes sign in the usual way.

The boundary operator $\partial_q : C_q(K) \rightarrow C_{q-1}(K)$ is defined on an oriented simplex by

$$\partial_q[v_0, \dots, v_q] = \sum_{i=0}^q (-1)^i [v_0, \dots, \widehat{v}_i, \dots, v_q],$$

where \widehat{v}_i indicates omission of the vertex v_i , and the map is extended linearly. The fundamental identity $\partial_{q-1}\partial_q = 0$ holds for all q , so the sequence

$$\dots \xrightarrow{\partial_{q+1}} C_q(K) \xrightarrow{\partial_q} C_{q-1}(K) \xrightarrow{\partial_{q-1}} \dots \xrightarrow{\partial_1} C_0(K) \rightarrow 0$$

forms a chain complex. The q -th homology group is then

$$H_q(K) = \ker(\partial_q) / \text{im}(\partial_{q+1}),$$

which records q -dimensional cycles modulo boundaries. In the present paper, this topological information will appear as the harmonic part of the Laplacian, while the nonzero spectrum will encode additional geometric and combinatorial structure.

When working with a filtration $K^{(0)} \subseteq K^{(1)} \subseteq \dots \subseteq K^{(T)}$, or more generally, with an inclusion of simplicial complexes $K \hookrightarrow L$, the corresponding chain groups and boundary operators are related by restriction to the appropriate simplex sets. This viewpoint will allow us to define persistent Laplacians in the next subsection.

2.2 Combinatorial Laplacians and Hodge decomposition

Given a simplicial complex K , we equip each chain group $C_q(K)$ with the standard Euclidean inner product in the oriented simplex basis. With respect to this inner product, the adjoint of the boundary operator $\partial_q : C_q(K) \rightarrow C_{q-1}(K)$ is the map $\partial_q^* : C_{q-1}(K) \rightarrow C_q(K)$. In matrix form, if B_q denotes the boundary matrix, then ∂_q^* is represented by B_q^\top .

The *combinatorial q -Laplacian* is defined by

$$\Delta_q = \partial_{q+1}\partial_{q+1}^* + \partial_q^*\partial_q.$$

The elements of $\ker(\Delta_q)$ are the *harmonic q -chains*. A basic consequence of discrete Hodge theory is that harmonic chains represent homology classes, and indeed, there is a canonical isomorphism

$$\ker(\Delta_q) \cong H_q(K).$$

Thus, the zero eigenspace of the combinatorial Laplacian recovers the topological information encoded by q -dimensional homology.

The harmonic component detects persistent topological features, while the positive eigenvalues measure how q -simplices interact through the complex.

2.3 Persistent Laplacians

Persistent homology tracks which homological features of a smaller complex remain visible inside a larger one. Let $X \subseteq Y$ be simplicial complexes, for example two scales $X = K^{(s)}$ and $Y = K^{(t)}$ in a filtration with $s \leq t$. Intuitively, the q -dimensional persistent homology of the (filtration) pair (X, Y) consists of those q -cycles in X that remain nontrivial when viewed inside Y . Formally,

$$H_q^{X,Y} := \ker(\partial_q^X) / (\text{im}(\partial_{q+1}^Y) \cap C_q(X)).$$

To define the corresponding persistent Laplacian, one restricts attention to those $(q+1)$ -chains in Y whose boundary lies in $C_q(X)$. Specifically, define

$$C_{q+1}^{X,Y} := \{c \in C_{q+1}(Y) : \partial_{q+1}^Y c \in C_q(X)\},$$

and let $\partial_{q+1}^{X,Y} : C_{q+1}^{X,Y} \rightarrow C_q(X)$ denote the restriction of ∂_{q+1}^Y to this subspace. Since $C_{q+1}^{X,Y}$ inherits an inner product from $C_{q+1}(Y)$, the adjoint

$$(\partial_{q+1}^{X,Y})^* : C_q(X) \rightarrow C_{q+1}^{X,Y}$$

is well defined. The q -th persistent Laplacian is then

$$\Delta_q^{X,Y} = \partial_{q+1}^{X,Y} (\partial_{q+1}^{X,Y})^* + (\partial_q^X)^* \partial_q^X.$$

The key structural fact is the persistent Hodge theorem: $\ker(\Delta_q^{X,Y}) \cong H_q^{X,Y}$. Thus, the harmonic sector of the persistent Laplacian recovers exactly the persistent homological information of the pair. In particular, the multiplicity of the zero eigenvalue is the persistent Betti number. This can be understood as the definition of persistent homology. When $X = Y$, this reduces to the ordinary combinatorial Laplacian and ordinary homology.

2.4 Spectral gap

Denote the eigenvalues $0 \leq \lambda_{q,1}^{X,Y} \leq \lambda_{q,2}^{X,Y} \leq \dots \leq \lambda_{q,n_q}^{X,Y}$ of the persistent q -Laplacian $\Delta_q^{X,Y}$ listed in nondecreasing order and repeated according to multiplicity. Since $\Delta_q^{X,Y}$ is symmetric and positive semidefinite, all eigenvalues are real and nonnegative. Let

$$m = \dim \ker(\Delta_q^{X,Y}) = \beta_q^{X,Y}$$

denote the persistent Betti number. Then $\lambda_{q,1}^{X,Y} = \dots = \lambda_{q,m}^{X,Y} = 0$ when $m > 0$, while $\lambda_{q,1}^{X,Y} > 0$ when $m = 0$. We define the *spectral gap* of $\Delta_q^{X,Y}$ to be

$$\gamma_q^{X,Y} := \min\{\lambda > 0 : \lambda \in \text{spec}(\Delta_q^{X,Y})\},$$

provided that $\Delta_q^{X,Y}$ has at least one positive eigenvalue. Equivalently, if $m < n_q$, then $\gamma_q^{X,Y} = \lambda_{q,m+1}^{X,Y}$. Thus the spectral gap is the smallest nonzero eigenvalue of the persistent Laplacian.

2.5 Analytic torsion

For more details, we refer the reader to Mnev (2014). The spectral gap isolates only the first positive eigenvalue of the persistent Laplacian. To summarize the rest of the non-harmonic spectrum, we use a determinant-type spectral statistic derived from analytic torsion.

Let $\lambda_{q,1}^{X,Y} \leq \lambda_{q,2}^{X,Y} \leq \dots \leq \lambda_{q,n_q}^{X,Y}$ be the eigenvalues of the persistent q -Laplacian $\Delta_q^{X,Y}$, and let

$$m_q = \dim \ker(\Delta_q^{X,Y})$$

be the persistent Betti number in degree q . We define the (log-)pseudodeterminant of $\Delta_q^{X,Y}$ by

$$\log \det_0(\Delta_q^{X,Y}) = \sum_{\lambda \in \text{spec}(\Delta_q^{X,Y}), \lambda > 0} \log \lambda.$$

Thus, zero eigenvalues do not contribute to the pseudodeterminant; they are excluded rather than regularized or perturbed. This is the finite-dimensional analog of taking the determinant over the non-harmonic sector only.

Using these pseudodeterminants, a discrete torsion statistic may be defined by the alternating product

$$\log T(X, Y) = \frac{1}{2} \sum_{q \geq 0} (-1)^{q+1} q \log \det_0(\Delta_q^{X,Y}).$$

This is the natural finite-dimensional torsion-style summary associated with the persistent Laplacians of the pair (X, Y) .

For a (weighted) graph G , the definition of torsion reduces to the notion of graph determinant (note that we removed the factor of q)

$$\log T_G(X, Y) = \log \det_0(\Delta_0^{X,Y}).$$

By Kirchhoff’s theorem $\frac{1}{n_0 - m_0 + 1} \log T_G(G, G)$ counts the number of spanning trees in G . In this zero-dimensional setting, $\Delta_0^{G,G}$ agrees with the standard definition of a graph Laplacian using the difference of degree and adjacency matrices. See Moore and Mertens (2011) for details.

3 Experimental Setup

Using the mathematics that we have introduced, we explain our feature extraction from Laplacians.

3.1 Feature construction

We construct our feature vectors as follows. For each filtration pair, we append the Betti numbers in all homological dimensions, the spectral gaps in all homological dimensions, and the analytic torsion (we use the logarithmic form for computational stability) to the corresponding feature vector. In practice, this gets modified slightly depending on the dataset, as explained in the next section.

3.2 Benchmark datasets

To demonstrate the universal nature of analytic torsion and spectral gap as primary features driving persistent Laplacians, we examine how the features provide advantage across a broad spectrum of benchmarking data sets. The datasets are chosen to demonstrate the efficiency of our feature vectors across 1, 2, and 3-dimensional data. We briefly describe the experimental setup for each dataset. The detailed description of how the persistent Laplacians are constructed from the relevant dataset can be found in the corresponding papers, whose code is openly available (see Section 6).

SKEMPI WT(wild-type) dataset provides the baseline binding affinity and structural data for 343 unmutated protein-protein complexes. It is a subset of the comprehensive SKEMPI v2 dataset (CC BY 4.0) Moal and Fernández-Recio (2012); Jankauskaitė et al. (2018), which catalogs thermodynamic and kinetic data for thousands of mutated protein interactions. The data is used to predict the binding energy of the protein-protein interactions, values in our work are in kcal/mol. Importantly for our application, the raw data includes spatial positions and names of elements on the binding interface.

We construct Rips and Alpha complexes from the data Edelsbrunner and Mücke (1994); Vietoris (1927) and extract features from those using standard approaches, see Xu et al. (2025). We keep those features untouched. Additionally, we construct the persistent graph Laplacians and extract the zeroth Betti number, the spectral gap, and the graph torsion. We also extract the first Betti number using the two different interpretations of the Euler characteristic of the graph. Hence, the contribution to the feature vector from the Laplacian is four-dimensional. The original feature vector consisted of eight statistical quantities.

MNIST (GNU GPL v3.0) LeCun et al. (1998) is a benchmark computer vision dataset containing 70,000 grayscale 28×28 images of handwritten digits. The data is used for training models on image (in this case number) recognition. We process the images using a single height filtration and by reducing the images from grayscale to black and white, as in Davies et al. (2023). Persistent Laplacians are formed from cubical complexes in dimension 0 and 1. This corresponds to the fact

that persistent homology becomes trivial in dimensions equal to or higher than the dimensions of the object.

From the spectral data we extract $2 \cdot 2 + 1$ dimensional feature vectors. These features are precisely those described at the beginning of this section. The original feature vectors had length $2 \cdot 10$ (for 10 eigenvalues in 2 dimensions).

QM-3D is a roughly 7,000 element subset of the larger dataset MoleculeNet (MIT license) Rupp et al. (2012); Blum and Raymond (2009); Wu et al. (2018). The subset that we use consists of position vectors of each element in a molecule. Other versions include additional information about the molecule or the atoms. The data is used for predicting the energy of the molecules measured in kcal/mol. The data comes with an official P -matrix split for the training and testing data. Using the Rips complex Vietoris (1927), we obtain a simplicial complex from which we construct the persistent Laplacians.

From the spectral data, we extract $3 \cdot 2 + 1$ dimensional feature vectors. These features are precisely those described at the beginning of this section. The original feature vectors had length $3 \cdot 10$ (for 10 eigenvalues in 3 dimensions).

3.3 Learning protocols

For the MNIST recognition task, we train our model using RandomForestClassifier (with 5 folds) from the Python package scikit-learn. For the estimation tasks of the QM-3D dataset, we use the RandomForestRegressor (with 5 folds) model from the same Python package. For the SKEMPI WT dataset, we use the GradientBoostingRegressor (with 10 folds to match Xu et al. (2025)) model from the Python package scikit-learn (this corresponds to the PLD-Tree method of Xu et al. (2025)). We use a fixed seed when comparing the results with those obtained using feature vectors from Davies et al. (2023); Xu et al. (2025). We do not scale our feature vectors in order to present the ideas in and of themselves.

4 Benchmark Results

We compare our feature vectors to the original methods of Davies et al. (2023); Xu et al. (2025). We expect analogous results to hold for other models and datasets, which use feature vectors built from (persistent) combinatorial Laplacians.

4.1 Main predictive performance

Table 1 presents a comparison between our computational results and the computational results of (Davies et al., 2023, Table 1) and (Xu et al., 2025, Table 3, PLD-tree column). We use the same quantities for measuring the accuracy as in the original papers.

Table 1: Main predictive performance: comparison of our compressed topological-spectral representation against baseline full-spectrum or statistical methods from (Davies et al., 2023, Table 1) and (Xu et al., 2025, Table 3, PLD-tree column). Bold values indicate the best performance for each metric. Recall that the SKEMPI WT dataset uses features beyond just the spectral data.

Dataset	Evaluation Metric	Baseline	Our Features
MNIST	Classification Accuracy	85.4%	86.2%
QM-3D	Mean Absolute Error	52.2	53.1
SKEMPI WT*	Mean Absolute Error	1.70	1.67
SKEMPI WT*	Pearson Correlation	0.66	0.67

4.2 Ablation study

SHAP Feature importance analysis Lundberg and Lee (2017) was run on the models using our feature vectors for the MNIST and QM-3D datasets. The analysis showed that the model strongly favored spectral gap and torsion for learning on the QM-3D dataset, and spectral gap and Betti numbers for learning on the MNIST dataset. This shows that all features used contribute to the effectiveness of

the feature vector, which can also be confirmed by running a model on only a subset of the features. Table 2 presents the performance of the model on chosen subsets of our features (see Appendix A).

5 Discussion

5.1 Stability and Robustness

The stability of topological descriptors under noise is a central concern in topological data analysis. While persistent homology benefits from well-known stability results, the spectral properties of the persistent Laplacian offer a distinct form of geometric robustness. Analytic torsion, by aggregating the entire non-harmonic spectrum into a single determinant-type quantity, acts as a global summary that is inherently less sensitive to the noise of individual high-frequency eigenvalues. In our benchmarks, this mathematical feature engineering preserves critical signal while bypassing the threshold where increasing raw eigenvalue counts typically leads to diminished model precision.

5.2 Computational Efficiency

Our proposed feature vectors tend to be low-dimensional, at the very least halving the length of the existing feature vectors. This lower dimensionality significantly mitigates the risk of overfitting and avoids the “breaking point” where high-frequency noise hinders model precision Davies et al. (2023). Additionally, This leads to shorter training times, reduced computational overhead, and memory footprint required for large-scale datasets. See the Appendix B for timing results.

5.3 Limitations and the Global-Local Tradeoff

It is important to acknowledge that analytic torsion is a global invariant. While it effectively summarizes how geometric “twisting” and connectivity evolve across a filtration, it does so by compressing the higher-frequency information into a single scalar. For tasks that depend on highly localized geometric primitives or specific oscillatory modes, the raw non-harmonic spectrum may still contain discriminative information that torsion aggregates away. However, our empirical results suggest that for a wide range of benchmarks in molecular physics and computer vision, this global-local tradeoff strongly favors the compact spectral representation over raw spectral data.

6 Conclusion

Persistent Laplacians significantly enrich topological data analysis by incorporating non-harmonic spectral information that captures the geometric evolution of filtered complexes. In this work, we have demonstrated that this vast spectral channel can be effectively concentrated into a compact, tripartite feature set: Betti numbers, spectral gaps, and analytic torsion.

Across benchmark datasets, our proposed representation performs comparably to the full persistent-Laplacian eigenspectrum and consistently outperforms the statistical summaries used in previous studies. By providing a mathematically principled and fixed-length interface, we eliminate the manual optimization and heuristic guesswork typically associated with spectral feature engineering.

This work establishes a transparent framework for characterizing how shape and connectivity evolve across a filtration, effectively bridging the gap between classical spectral geometry and modern topological learning. Future directions will include the investigation of sheaf-based persistent Laplacians Jones and Wei (2026); Wang and Wei (2026); Wei and Wei (2025a) and the stability of these invariants under varying noise regimes, in line with Peek et al. (2025); Jung et al. (2025).

Data and Software Availability

The source code used for these benchmarks was modified from <https://github.com/tomogwen/persistentlaplaciandatasience> (MIT license) and <https://github.com/xxjan719/PLNet> (MIT license), corresponding to Davies et al. (2023); Xu et al. (2025) respectively. The modified code will be made available upon request. The raw datasets are sourced from their respective official repositories as cited in Section 3.

Acknowledgments and Disclosure of Funding

A.D.L. and J.G. were partially supported by NSF grants DMS-1902092 and DMS-2200419, and the Simons Foundation collaboration grant on New Structures in Low-dimensional Topology. Computations associated with this project were conducted utilizing the Center for Advanced Research Computing (CARC) at the University of Southern California. We would like to thank H. J. Arai for helpful conversations.

References

- H. Adams, T. Emerson, M. Kirby, R. Neville, C. Peterson, P. Shipman, S. Chepushtanova, E. Hanson, F. Motta, and L. Ziegelmeier. 2017. Persistence images: A stable vector representation of persistent homology. *Journal of Machine Learning Research* 18, 1 (2017), 218–252.
- M. Belkin and P. Niyogi. 2003. Laplacian Eigenmaps for Dimensionality Reduction and Data Representation. *Neural Computation* 15, 6 (2003), 1373–1396. <https://doi.org/10.1162/089976603321780317>
- L. C. Blum and J.-L. Reymond. 2009. 970 Million Druglike Small Molecules for Virtual Screening in the Chemical Universe Database GDB-13. *Journal of the American Chemical Society* 131, 25 (June 2009), 8732–8733. <https://doi.org/10.1021/ja902302h>
- P. Bubenik. 2015. Statistical topological data analysis using persistence landscapes. *Journal of Machine Learning Research* 16, 1 (2015), 77–102.
- G. Carlsson. 2009. Topology and data. *Bull. Amer. Math. Soc.* 46, 2 (Jan. 2009), 255–308. <https://doi.org/10.1090/s0273-0979-09-01249-x>
- F. Chazal, B. T. Fasy, F. Lecci, A. Rinaldo, and L. Wasserman. 2015. Stochastic convergence of persistence landscapes and silhouettes. *Journal of Computational Geometry* 6, 1 (2015), 140–161.
- J. Cheeger. 1979. Analytic Torsion and the Heat Equation. *Annals of Mathematics* 109, 2 (1979), 259–321. <https://doi.org/10.2307/1971113>
- D. Chen, J. Liu, J. Wu, and G.-W. Wei. 2023. Persistent hyperdigraph homology and persistent hyperdigraph Laplacians. *Foundations of Data Science* 5, 4 (2023), 558–588. <https://doi.org/10.3934/fods.2023010>
- J. Chen, Y. Qiu, R. Wang, and G.-W. Wei. 2022. Persistent Laplacian projected Omicron BA.4 and BA.5 to become new dominating variants. *Computers in Biology and Medicine* 151 (Dec. 2022), 106262. <https://doi.org/10.1016/j.combiomed.2022.106262>
- F. R. K. Chung. 1997. *Spectral Graph Theory*. CBMS Regional Conference Series in Mathematics, Vol. 92. American Mathematical Society, Providence, RI.
- R. R. Coifman, S. Lafon, A. B. Lee, M. Maggioni, B. Nadler, F. Warner, and S. W. Zucker. 2005. Geometric Diffusions as a Tool for Harmonic Analysis and Structure Definition of Data: Diffusion Maps. *Proceedings of the National Academy of Sciences* 102, 21 (2005), 7426–7431. <https://doi.org/10.1073/pnas.0500334102>
- T. Davies, Z. Wan, and R. J. Sanchez-Garcia. 2023. The Persistent Laplacian for Data Science: Evaluating Higher-Order Persistent Spectral Representations of Data. In *Proceedings of the 40th International Conference on Machine Learning (Proceedings of Machine Learning Research, Vol. 202)*. PMLR, 7249–7263. <https://proceedings.mlr.press/v202/davies23c.html>
- B. Eckmann. 1945. Harmonische Funktionen und Randwertaufgaben in einem Komplex. *Commentarii Mathematici Helvetici* 17 (1945), 240–255. <https://doi.org/10.1007/BF02566245>
- H. Edelsbrunner, D. Letscher, and A. Zomorodian. 2002. Topological Persistence and Simplification. *Discrete & Computational Geometry* 28, 4 (2002), 511–533. <https://doi.org/10.1007/s00454-002-2885-2>

- H. Edelsbrunner and E. P. Mücke. 1994. Three-dimensional alpha shapes. *ACM Transactions on Graphics* 13, 1 (Jan. 1994), 43–72. <https://doi.org/10.1145/174462.156635>
- M. Fiedler. 1973. Algebraic Connectivity of Graphs. *Czechoslovak Mathematical Journal* 23, 2 (1973), 298–305. <https://doi.org/10.21136/CMJ.1973.101168>
- C. Gordon, D. L. Webb, and S. Wolpert. 1992. One Cannot Hear the Shape of a Drum. *Bull. Amer. Math. Soc.* 27, 1 (1992), 134–138. <https://doi.org/10.1090/S0273-0979-1992-00289-6>
- J. Jankauskaitė, B. Jiménez-García, J. Dapkūnas, J. Fernández-Recio, and I. H. Moal. 2018. SKEMPI 2.0: an updated benchmark of changes in protein–protein binding energy, kinetics and thermodynamics upon mutation. *Bioinformatics* 35, 3 (07 2018), 462–469. <https://doi.org/10.1093/bioinformatics/bty635>
- B. Jones and G.-W. Wei. 2026. PETLS: PERSISTENT TOPOLOGICAL LAPLACIAN SOFTWARE. arXiv:2508.11560 [math.AT] <https://arxiv.org/abs/2508.11560>
- I. Jung, W. Kang, and H. Park. 2025. Persistent Laplacian Diagrams. arXiv:2512.05463 [math.AT] <https://arxiv.org/abs/2512.05463>
- M. Kac. 1966. Can One Hear the Shape of a Drum? *The American Mathematical Monthly* 73, 4P2 (1966), 1–23. <https://doi.org/10.1080/00029890.1966.11970915>
- Y. LeCun, C. Cortes, and C. C. J. Burges. 1998. The MNIST Handwritten Digit Database. Yann LeCun’s Website. <http://yann.lecun.com/exdb/mnist/> Archived from the original on 2020-04-30.
- Z. Li, M. Qi, J. Huang, W. Zhang, X. Tan, and Y. Chen. 2025. Geometry-enhanced graph neural networks accelerate circRNA therapeutic target discovery. *Frontiers in Genetics* 16 (2025), 1633391. <https://doi.org/10.3389/fgene.2025.1633391>
- S. M. Lundberg and S.-I. Lee. 2017. A Unified Approach to Interpreting Model Predictions. In *Neural Information Processing Systems*. <https://api.semanticscholar.org/CorpusID:21889700>
- P. Mnev. 2014. Lecture notes on torsions. arXiv:1406.3705 [math.AT] <https://arxiv.org/abs/1406.3705> arXiv:1406.3705.
- I. H. Moal and J. Fernández-Recio. 2012. SKEMPI: a Structural Kinetic and Energetic database of Mutant Protein Interactions and its use in empirical models. *Bioinformatics* 28, 20 (Aug. 2012), 2600–2607. <https://doi.org/10.1093/bioinformatics/bts489>
- C. Moore and S. Mertens. 2011. The Nature of Computation. Oxford University Press, 1–14.
- W. Müller. 1978. Analytic Torsion and R -Torsion of Riemannian Manifolds. *Advances in Mathematics* 28, 3 (1978), 233–305. [https://doi.org/10.1016/0001-8708\(78\)90116-0](https://doi.org/10.1016/0001-8708(78)90116-0)
- F. Mémoli, Z. Wan, and Y. Wang. 2022. Persistent Laplacians: Properties, Algorithms and Implications. *SIAM Journal on Mathematics of Data Science* 4, 2 (June 2022), 858–884. <https://doi.org/10.1137/21m1435471>
- D. Peek, M. P. Skerritt, and S. Chalup. 2025. Noise-Robust Topology Estimation of 2D Image Data via Neural Networks and Persistent Homology. In *AI 2025: Advances in Artificial Intelligence: 38th Australasian Joint Conference on Artificial Intelligence, AI 2025, Canberra, ACT, Australia, December 1–5, 2025, Proceedings, Part I* (Canberra, ACT, Australia). Springer-Verlag, Berlin, Heidelberg, 392–404. https://doi.org/10.1007/978-981-95-4969-6_30
- D. B. Ray and I. M. Singer. 1971. R -Torsion and the Laplacian on Riemannian Manifolds. *Advances in Mathematics* 7, 2 (1971), 145–210. [https://doi.org/10.1016/0001-8708\(71\)90045-4](https://doi.org/10.1016/0001-8708(71)90045-4)
- K. Reidemeister. 1935. Homotopieringe und Linsenräume. *Abhandlungen aus dem Mathematischen Seminar der Universität Hamburg* 11, 1 (Dec. 1935), 102–109. <https://doi.org/10.1007/bf02940717>

- M. Rupp, A. Tkatchenko, K.-R. Müller, and O. A. von Lilienfeld. 2012. Fast and Accurate Modeling of Molecular Atomization Energies with Machine Learning. *Physical Review Letters* 108, 5 (Jan. 2012). <https://doi.org/10.1103/physrevlett.108.058301>
- M. T. Schaub, A. R. Benson, P. S. Horn, G. Lippner, and A. Jadbabaie. 2020. Random Walks on Simplicial Complexes and the Normalized Hodge 1-Laplacian. *SIAM Rev.* 62, 2 (2020), 353–391. <https://doi.org/10.1137/18M1201019>
- C. Shen, X. Liu, J. Luo, and K. Xia. 2025. Torsion Graph Neural Networks. *IEEE Transactions on Pattern Analysis and Machine Intelligence* 47, 4 (2025), 2946–2956. <https://doi.org/10.1109/TPAMI.2024.3412589>
- L. Vietoris. 1927. Über den höheren Zusammenhang kompakter Räume und eine Klasse von zusammenhangstreuen Abbildungen. *Math. Ann.* 97, 1 (Dec. 1927), 454–472. <https://doi.org/10.1007/bf01447877>
- R. Wang, D. D. Nguyen, and G.-W. Wei. 2020. Persistent Spectral Graph. *International Journal for Numerical Methods in Biomedical Engineering* 36, 9 (2020), e3376. <https://doi.org/10.1002/cnm.3376>
- R. Wang and G.-W. Wei. 2023. Persistent path Laplacian. *Foundations of Data Science* 5, 1 (2023), 26–55. <https://doi.org/10.3934/fods.2022015>
- X. X. Wang and G.-W. Wei. 2026. Multi-dimensional Persistent Sheaf Laplacians for Image Analysis. arXiv:2602.14846 [cs.CV] <https://arxiv.org/abs/2602.14846>
- X. Wei and G.-W. Wei. 2025a. Persistent sheaf Laplacians. *Foundations of Data Science* 7, 2 (2025), 446–463. <https://doi.org/10.3934/fods.2024033>
- X. Wei and G.-W. Wei. 2025b. Persistent Topological Laplacians—A Survey. *Mathematics* 13, 2 (2025), 208. <https://doi.org/10.3390/math13020208>
- Z. Wu, B. Ramsundar, E. N. Feinberg, J. Gomes, C. Geniesse, A. S. Pappu, K. Leswing, and V. Pande. 2018. MoleculeNet: a benchmark for molecular machine learning. *Chemical Science* 9, 2 (2018), 513–530. <https://doi.org/10.1039/c7sc02664a>
- X. Xu, C. Wang, G.-W. Wei, and J. Chen. 2025. Persistent Laplacian neural network for protein–protein binding free energy prediction. *Protein Science* 34, 12 (Nov. 2025). <https://doi.org/10.1002/pro.70377>
- A. Zia and F. Hazratian. 2026. Representation Geometry as a Diagnostic for Out-of-Distribution Robustness. arXiv:2602.03951 [cs.LG] <https://arxiv.org/abs/2602.03951>

A Performance on subsets of features

This appendix is meant as supporting material to Section 4.2. We provide the evaluation of the model on only a subset of our features as well as on the statistical spectral data from Xu et al. (2025). The results suggest that all of our chosen features contribute to the final feature vector and they have different performance on the different tasks.

Table 2: Performance of the model on subsets of our features for MNIST and QM-3D datasets, and on the statistical feature vectors. The numbers in the MNIST column represent average percentages of correct predictions, and those in the QM-3D column show the mean absolute error in energy prediction.

Features	MNIST	QM-3D
Spectral gap	74.2%	62.1
Torsion	49.0%	60.2
Betti numbers	69.0%	170.8
Spectral gap and Betti numbers	85.2%	61.4
Spectral gap and torsion	77.0%	53.7
Betti numbers and torsion	77.1%	57.2
Statistical spectral data as in Xu et al. (2025)	78.8%	53.1

B Exact training times

This appendix is meant as supporting material to 5.2. We present the measurements of the total training time required on a single core of a laptop AMD Ryzen 9 8940HX, see Table 3, demonstrating speedups across the board. The time required for data preparation can be found in Davies et al. (2023); Xu et al. (2025), and remains largely unchanged by construction.

Table 3: Total training times for models as described in Section 3.3 on a single laptop core. Recall that we incorporated data beyond the spectrum to the SKEMPI WT feature vectors, hence offering lesser time improvement.

Dataset	Baseline Davies et al. (2023); Xu et al. (2025)	Our features
QM-3D (5-fold)	143.6s	24.9s
MNIST (5-fold)	12.6s	3.9s
SKEMPI WT* (10-fold)	284.3s	242.5s